Available online at www.sciencedirect.com

ScienceDirect

Procedia Structural Integrity 33 (2021) 51–58

Structural Integrity Procedia

www.elsevier.com/locate/procedia

IGF26 - 26th International Conference on Fracture and Structural Integrity

Design and Analysis of Mesh Size Subjected to Wheel Rim Convergence Using Finite Element Method

Yuwana Sanjaya[a], Aditya Rio Prabowo[a,*], Fitrian Imaduddin[a], Nur Azmah Binti Nordin[b]

[a]*Department of Mechanical Engineering, Universitas Sebelas Maret, Surakarta 57126, Indonesia*
[b]*Malaysia-Japan International Institute of Technology - Universiti Teknologi Malaysia, Kuala Lumpur 54100, Malaysia*

Abstract

This paper discusses the effect of meshing size on wheel rim. It is not known that every design needs to consider the optimum result of the design, in reality the simulation cannot generates the optimal analysis due to several factors. One of the influencing factors in the simulation is the mesh size when simulating the wheel rim design. It is known that each mesh size gives different results, therefore it is necessary to do a calibration using finite element method from the benchmarking literature studies that have discussed this case before. Authors designed a vehicle wheel using Fusion360 and ran the simulating static analysis using ANSYS. The material used is steel and the boundary conditions of its design is angular velocity and load. The wheel designs were given different mesh sizes and resulted in stress (von-Mises) and displacement, since the results were analyzed for mesh convergence. For the convergence result, wheel rim has a von-Mises stress for 10 mm, 15 mm, and 20 mm size mesh is 164.38 MPa, 128.68 MPa, and 131.08 MPa, and the displacement is 0.16117 mm, 0.15592 mm, 0.15286 mm. The simulation made stress ratio for 1.174, 0.919, 0.936 and displacement ratio for 0.989, 0.957, 0.938. Through the use of different mesh sizes, different results can be proven, this is necessary to determine the convergence of the mesh used in the simulation. This paper proves that 10, 15, 20 mm size mesh convergence, with error ratio of displacement is 0.011, 0.043, 0.062 and the error ratio of stress is -0.174, 0.081, 0.064 to the benchmarking studies literature.

Keywords: Wheelrim; Ansys; Convergent; mesh size, static analysis, finite element method;

* Corresponding author. Tel.: +62-271-632-163 ; fax: +62-271-623-163 .
E-mail address: aditya@ft.uns.ac.id

10.1016/j.prostr.2021.10.008

1. Introduction

Automobile wheel construction has progressed through the decades, from early spoke designs of wood and steel wheels used in horse-drawn carriages and bicycle technology, to flat steel disks, stamped metal configurations, and the newest generation of cast and forged aluminum alloy wheels, as reported by Igbudu and Fadare (2015). Nowadays, the use of vehicles is very important for life, because the need for high mobility makes the need for vehicles to increase. One of the important components in a vehicle is the wheel rim. Wheel rim is very important because without it, the vehicle cannot run. According to Karuppusamy et al. (2016), rim wheel is one of the most important structural components of vehicle tire assemblies, wheel rim connects the vehicle body and the tire and enables the wheel rotation. Durability assessment of mechanical components early in the design phase plays a key role in the automotive industries. Traditionally, this was primarily conducted with sample testing under the Actual operation conditions or through simulation tests with digitally operated servo-hydraulic equipment/tools (Wright, 1993; Dabit et al., 2020).

Finite element analysis (FEA) is a very common method used to evaluate any model that has been developed to provide technical estimation regarding structural performances, e.g., subjected to static and dynamic loadings (Kharmanda et al., 2016; Ary et al., 2020; Caesar et al., 2020; Ikhsan et al., 2020; Ridwan et al., 2020; Prabowo et al., 2020). Chen et al. (2017) asserted that the numerical simulation based on the finite element approach is a useful technique in the field of design. This simulation starts with making geometry with Fusion360 and continues with static simulation on ANSYS. Das (2014) has been mentioned that Passing through checks such as the radial test is the most common technique for car wheels. The boundary condition for the wheel rim simulated in this paper is radial force from the diameter of the wheel rim.

The results obtained are convergence between stress results (von-Mises, see Muttaqie et al., 2019 and Prabowo et al., 2019) and displacement simulation with benchmarking journals. In this case, proper mesh refinement (and mesh convergence analysis) is critical in determining the structure's safety (Ghavidel et al., 2020). Following that result, this paper will show the error ratio from the displacement ratio and stress ratio.

This paper continues to focus on an optimal design of rim wheel. Rim wheel that has been simulated also act as vehicle support. It is important for researchers to conduct a mesh convergence study before creating a model in order to obtain the required meshing size, as this can result in significant variations in the output (Ahmad et al., 2013). In case of mesh convergence study in ANSYS, Shah (2002) presented techniques to evaluate mesh convergence errors. The mesh convergence errors enable to monitor whether the numerical solution is reasonably correct even though the exact solution is not known (Bespalov, 2017).

The aim of this study is to perform a mesh convergence study for benchmarking of rim wheel. This paper using differences of mesh size on the simulation. Different types of loading conditions that can be used to determine the stress and displacement distributions on the wheel are discussed in this research work (Nallusamy et al., 2015). In finite element analysis, the accuracy of the result obtained is determined by size of the mesh. According to the theory of the finite element analysis, finite modal with small element size yields high accuracy as compared to the modal with large element size. Also, if the size of the element is large then complexity of the modal increases, it is only used where high accuracy is required. From the parameters, Error ratio can be obtained to prove that mesh size affects the results of simulation. The appropriate approach must be well prepared and considered before and during the analysis process in order to reach the aims and to solve all problems as stated by Mohamad et al (2017).

Nomenclature

E	Young's modulus
σ	Yield stress
δ	Density
E_{size}	Mesh size
$\overline{x}t$	Average thickness
Δx	Displacement
$\sigma_{v\text{-}M}$	Stress of the von-Mises
SF	Safety factor

2. FE Setting and Configuration

For this simulation using steel alloy as a material on the rim wheel. Alloy steels are those whose properties are owed primarily to the existence of an element or elements other than carbon, according to the definition of International Committee of the International Society for Testing Materials (Crook, 1927). Properties from steel that has been input for wheel rim static analysis using ANSYS. In this study, properties of steel are given as follows: Young's modulus $E = 2.34\times10^5$ N/mm^2; stress of the von-Mises $\sigma_{v\text{-}M}$ = 240 N/mm^2; and density δ = 7800 kg/m^3.

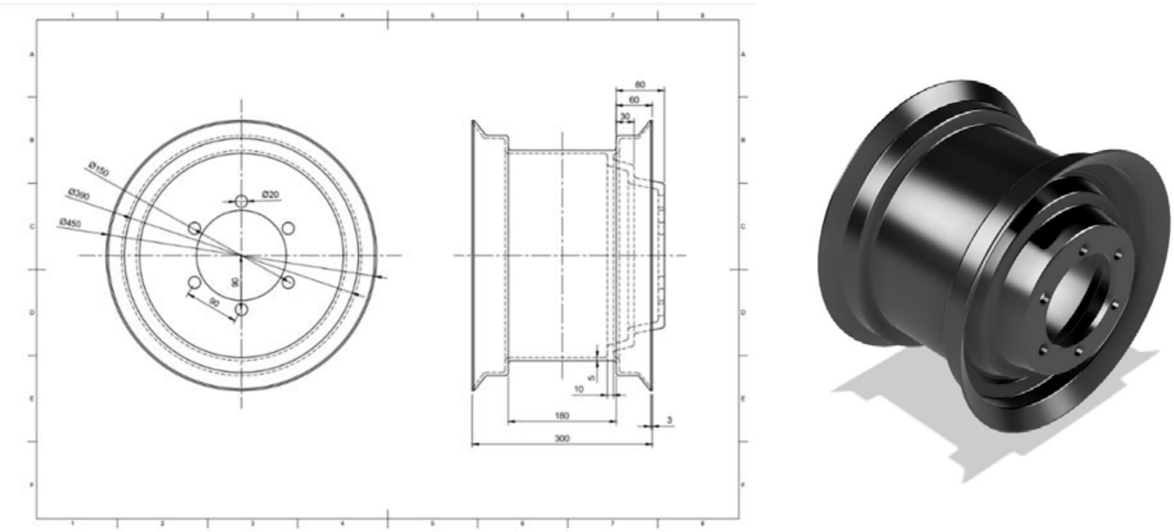

(a) (b)

Fig. 1. (a) 2D Geometry of the wheel rim model; (b) 3D design of the wheel rim.

The design of the wheel rim geometry uses the Fusion360, with dimensions at Fig. 1. (a). The design of the 3D wheel rim is showed in Fig. 1. (b). The geometry wheel rim design that has been designed in the Fusion360 is then imported to ANSYS, with different mesh sizes for each experiment. Selected target for mesh size are designated on same regions of the wheel rim body. The mesh size used is a multiple of 5 shown in Table 1, starting with mesh size of 10 mm, and ends with mesh size of 60 mm.

Table 1. Mesh size of the wheel rim model.

E_{size} (mm)	$\overline{X}t$ (mm)	E_{size} / $\overline{X}t$	Nodes	Elements
10	6	1.667	109303	54137
15	6	2.500	53013	26720
20	6	3.333	35613	17957
25	6	4.167	27005	13598
30	6	5.000	21262	10776
35	6	5.833	18338	9399
40	6	6.667	17194	8842
45	6	7.500	15844	8148
50	6	8.333	15103	7800
55	6	9.167	14476	7436
60	6	10.000	13991	7147

To get results that resemble comparative journals, it is necessary to equate the boundary conditions and loading in the Wheel rim simulation. With a load of 21.3 kN for each bolt holes. Displacement (translational and rotational in x, y, z direction is zero). Angular velocity (x, z direction is zero and y direction is 62.8 rad/s). The benchmarking reference is used as a comparison has a limit in the form of stress (von-Misses) and displacement shown in Table 2. Von-Mises stress values were obtained from ANSYS and number of cycles to failure was obtained.

Table 2. Benchmarking results of the wheel rim.

Material	Δx (mm)	$\sigma_{v\text{-}M}$ (MPa)
Steel Alloy	2.34×10^5	240

3. Result and Discussion

3.1. Displacement and stress ratio

The results of the displacement ratio of eleventh simulations shows varying displacement ratio that presented in Table 3. Ashford and Sitar (2001) Asserted that the finite element models estimated the displacement more accurately than the static simulation, which was due to the same explanation. The displacement ratio of the first variation rim wheel is 0.989. In the second, the displacement ratio is 0.957. In the third variation, the displacement ratio is 0.938. The fourth variation of the total displacement ratio is 0.914. The fifth variation has displacement ratio of 0.891. The sixth variation has a deformation of 0.868. In the seventh variation, the displacement ratio is 0.846. The eighth variation of the displacement ratio is 0.831. In the ninth variation, the displacement ratio is 0.833. The tenth variation of the displacement ratio is 0.797. In the last variation, the displacement ratio is 0.793.

Table 3. Displacement ratio of the wheel rim.

E_{size} (mm)	Nodes	Elements	Δx (mm)	Benchmark Δx (mm)	Ratio Δx
10	109303	54137	0.16117	0.163	0.989
15	53013	26720	0.15592	0.163	0.957
20	35613	17957	0.15286	0.163	0.938
25	27005	13598	0.14892	0.163	0.914
30	21262	10776	0.14517	0.163	0.891
35	18338	9399	0.14143	0.163	0.868
40	17194	8842	0.13785	0.163	0.846
45	15844	8148	0.13548	0.163	0.831
50	15103	7800	0.1357	0.163	0.833
55	14476	7436	0.12999	0.163	0.797
60	13991	7147	0.12933	0.163	0.793

The results of the stress ratio of eleventh simulations shows varying stress ratio that presented in Table 4. The aim of the study is to study about wheel rim stress failures and the forces that work on them (Sureddi, 2018). The stress ratio of the first variation rim wheel is 1.174. In the second, the stress ratio is 0.919. In the third variation, the stress ratio is 0.936. The fourth variation of the stress ratio is 0.892. The fifth variation has stress ratio of 0.898. The sixth variation has stress ratio of 0.839. In the seventh variation, the stress ratio is 0.830. The eighth variation of the stress ratio is 0.853. In the ninth variation, the stress ratio is 0.747. The tenth variation of the stress ratio is 0.827. In the last variation, the stress ratio is 0.803.

Table 4. Stress ratio of the wheel rim.

E_{size} (mm)	Nodes	Elements	$\sigma_{v\text{-}M}$ (MPa)	Benchmark $\sigma_{v\text{-}M}$ (MPa)	$\sigma_{v\text{-}M}$ Ratio
10	109303	54137	164.38	140.056	1.174
15	53013	26720	128.68	140.056	0.919
20	35613	17957	131.08	140.056	0.936
25	27005	13598	124.9	140.056	0.892
30	21262	10776	125.81	140.056	0.898
35	18338	9399	117.56	140.056	0.839
40	17194	8842	116.28	140.056	0.830
45	15844	8148	119.45	140.056	0.853
50	15103	7800	104.62	140.056	0.747
55	14476	7436	115.82	140.056	0.827
60	13991	7147	112.45	140.056	0.803

Convergence study represent graphically to Fig. 2. (a) where the displacement ratio that is close to convergence is the first variation at a mesh size of 10 mm with displacement ratio of 0.989, the nodes is 109303, and the elements is 54137. In the second variation, the mesh size of 15 mm has a displacement ratio of 0.919, the nodes is 53013, and the element is 26720. In the third variation, the mesh size of 20 mm has displacement ratio of 0.938, with the nodes is 35613, and the elements is 17957. Fig. 3. (a), Fig. 3. (b), and Fig. 3. (c) show the displacement profiles of each size mesh that convergence. The results are graphically presented in Fig. 2. (b). Convergence study represent graphically to Fig. 3 where the displacement ratio that is close to convergence is the first variation at a mesh size of 10 mm with displacement ratio of 1.174, the nodes is 109303, and the elements is 54137. In the second variation, the mesh size of 15 mm has a displacement ratio of 0.919, the nodes is 53013, and the element is 26720. In the third variation, the mesh size of 20 mm has displacement ratio of 0.936, with the nodes is 35613, and the elements is 17957. Fig. 4. (a), Fig. 4. (b) and Fig. 4. (c) show the displacement profiles of each size mesh that convergence.

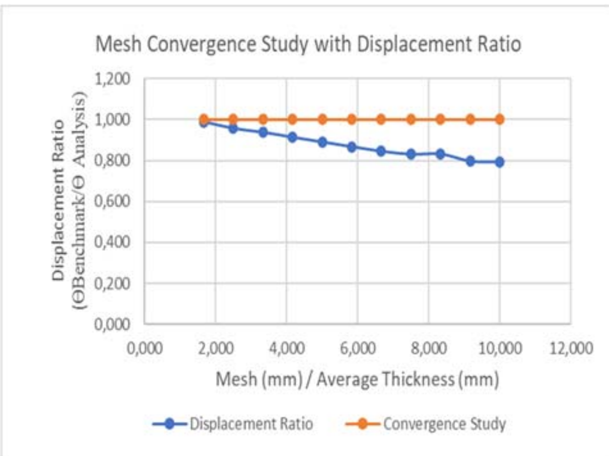

(a)

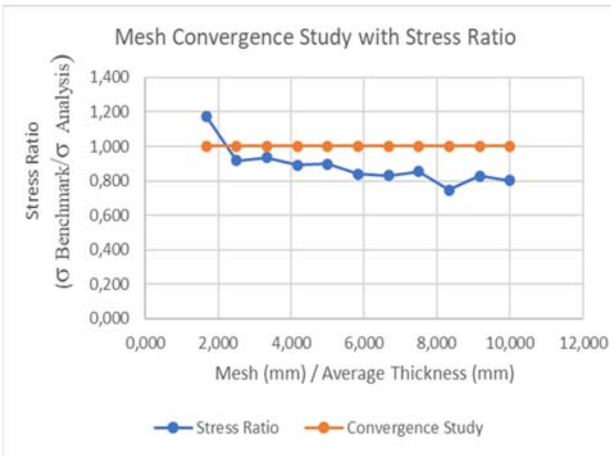

(b)

Fig. 2. (a) Mesh convergence study with displacement ratio; and (b) mesh convergence study with stress ratio.

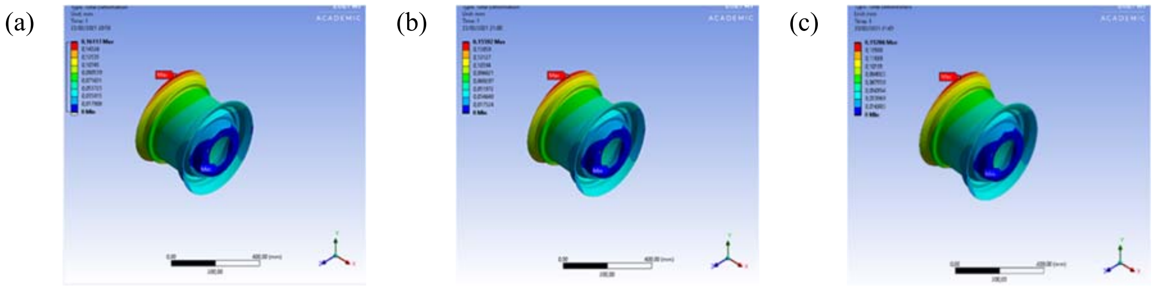

Fig. 3. (a) Displacement of Mesh Size 10 mm; (b) Displacement of Mesh Size 15 mm; (c) Displacement of Mesh Size 20 mm

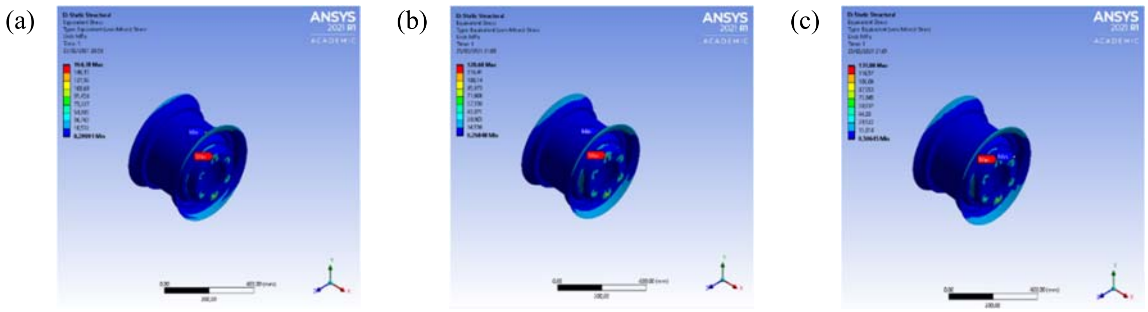

Fig. 4. (a) Stress of the mesh size 10 mm; (b) stress of the mesh size 15 mm; and (c) stress of the mesh size 20 mm.

3.2. Error ratio

Burr and Cheatham (1995) showed that safety factor used in automobiles is 3.0. All variations have average safety factor more than 14, this proves that the variations safe to use since the criterion safety factor is 3.0, as visible in Fig. 5. (a), Fig. 5. (b). and Fig. 5. (c). Error ratio is generally calculated by comparison of the ratio of displacement and the error ratio of stress with the benchmarking study of number of displacement and the number of stress, where the results are shown in Table 5.

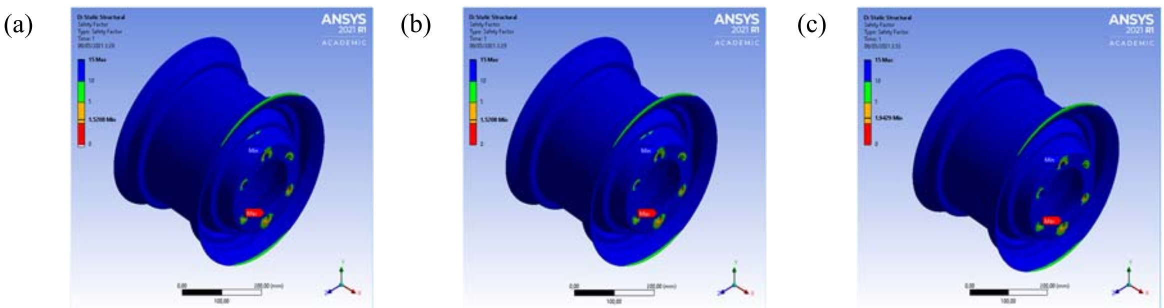

Fig. 5. (a) Safety factor of the mesh size 10 mm; (b) safety factor of the mesh size 15 mm; (c) safety factor of the mesh size 20 mm.

The error ratio of displacement (see Table 5) of the first variation rim wheel is 0.011 and the error ratio of stress is -0.174. In the second, the error ratio of displacement is 0.043 and the error ratio of stress is 0.081. In the third variation, the error ratio of displacement is 0.062 and the error ratio of stress is 0.064. The fourth variation of the error ratio of displacement is 0.086 and the error ratio of stress is 0.108. The fifth variation has error ratio of displacement of 0.109 and the error ratio of stress is 0.102. The sixth variation has error ratio of displacement of 0.132 and the error ratio of stress is 0.161. In the seventh variation, the error ratio of displacement is 0.154 and the error ratio of stress is 0.169.

The eighth variation of the error ratio of displacement is 0.169 and the error ratio of stress is 0.147. In the ninth variation, the error ratio of displacement is 0.167 and the error ratio of stress is 0.253. The tenth variation of the error ratio of displacement is 0.827 and the error ratio of stress is 0.173. In the last variation, the error ratio of displacement is 0.207 and the error ratio of stress is 0.197.

Table 5. Overall error ratio of the wheel rim analysis.

E_{Size} (mm)	$\overline{X}t$ (mm)	E_{Size} / $\overline{X}t$	*SF*	Error Ratio Δx	Error Ratio $\sigma_{v\text{-}M}$
10	6	1.667	14.703	0.011	-0.174
15	6	2.500	14.664	0.043	0.081
20	6	3.333	14.658	0.062	0.064
25	6	4.167	14.66	0.086	0.108
30	6	5.000	14.669	0.109	0.102
35	6	5.833	14.656	0.132	0.161
40	6	6.667	14.669	0.154	0.169
45	6	7.500	14.664	0.169	0.147
50	6	8.333	14.695	0.167	0.253
55	6	9.167	14.678	0.203	0.173
60	6	10.000	14.708	0.207	0.197
			Average	0.122	0.117
			Median	0.132	0.147
			Minimum	0.011	-0.174
			Maximum	0.207	0.253
			Standard of deviation	0.065	0.111
			Coefficient of variance	0.533	0.950

As depicted in Table 5, average error ratio refers to the sum of an error ratio divided by number of simulations, where the average error of displacement is 0.122 and the average error of stress is 0.011. Median error ratio is the value of error ratio separating the higher half from the lower half from number of simulations, where the median error of displacement is 0.132 and the median error of stress is 0.047. Minimum error ratio is the smallest error ratio value from number of simulations, where the minimum error ratio of displacement is 0.011 and the minimum error ratio of stress is -0.174. Max error ratio is the biggest error ratio from the number of simulations, where the max error ratio of displacement is 0.207 and the max error ratio of stress is 0.253. Standard of deviation error ratio is dispersion of error ratio from the number of simulations, Standard of deviation error ratio of displacement is 0.065 and the standard deviation error ratio of stress is 0.111. The coefficient of variation error ratio is the ratio of the standard deviation error ratio to the average error ratio, the coefficient of variation error ratio of displacement is 0.533 and the coefficient of variation error ratio of stress is 0.950.

4. Conclusions

Static analysis aims to determine the changes in displacement and von-Mises stress that occur from the study. Then, the value of displacements and stresses was evaluated using converged meshing sizes with variations in the parameters such as displacement ratio and stress ratio. From the above Table. 5, it has been proven that the mesh size affects the results of the simulation, it can be seen from the different simulation results for each mesh size. Convergence can be obtained from comparing each existing mesh size to simulate afterwards.

Based on the results, error percentage steel alloy material that is simulated has the closest results in the mesh size of 10 mm with the error displacement ratio of 0.011 and error stress ratio of -0.174. In the mesh size of 15 mm, with the error displacement ratio of 0.043 and error stress ratio of 0.081. In the mesh size 20 mm, with the error displacement ratio of 0.062 and error stress ratio of 0.064. The Error ratio of displacement has average for 0.122, the median is 0.132, the minimum is 0.011, the maximum is 0.207, the standard of deviation is 0.065, and the coefficient of variance is 0.533. At the same time, the error ratio of stress has average for 0.117, the median is 0.147, the minimum is -0.174, the maximum is 0.253, the standard of deviation is 0.111, and the coefficient of variance is 0.950.

From the coefficient error of variance, the lower the value of variation, the more precise the estimate and vice versa. Therefore, this convergence study gives evidence of the importance of mesh convergence and methods of estimation of discretization error. Effects of the mesh size can be seen from the smaller mesh size changes will made study results accurately. The optimization of the results of this analysis can be improved by comparing other materials from comparative journals with the same settings. By considering the mesh size, it is important to determine the mesh size ranges first, then determine the size of the mesh more detail. This will help the author to estimate the result of simulation more accurately.

References

Ahmad, M., Ismail, K.A., Mat, F., 2013. Convergence of finite element model for crushing of a conical thin-walled tube. Procedia Engineering 53, 586-593.

Ary, A.K., Prabowo, A.R., Imaduddin, F., 2020. Structural assessment of alternative urban vehicle chassis subjected to loading and internal parameters using finite element analysis. Journal of Engineering Science and Technology 15, 1999-2022.

Ashford, S.A., Sitar, N., 2001. Effect of element size on the static finite element analysis of steep slopes. International Journal for Numerical Analytical Methods in Geomechanics 25, 1361-1376.

Bespalov, A., Haberl, A., Praetorius, D,. 2017. Adaptive FEM with coarse initial mesh guarantees optimal convergence rates for compactly perturbed elliptic problems. Computer Methods in Applied Mechanics and Engineering 317, 318-340.

Burr, A., Cheatham, J., 1995. Mechanical design and analysis 2nd edition. Prentice-Hall. Section 5.2.

Caesar, B.P.P., Hazimi, H., Sukanto, H., Prabowo, A.R., 2020. Development of novel design and frame structural assessment on mitutoyo's auto checking hardness machine using reverse engineering approach: series hr-522 hardness tester. Journal of Engineering Science and Technology 15, 1296-1318.

Chen, L., Li, S., Chen, H., Saylor, D., Tong, S., 2017. Study on the design method of equal strength rim based on stress and fatigue analysis using finite element method. Advances in Mechanical Engineering 9, 1-11.

Crook, W.J., 1927. Alloy steels and their uses. Journal of Chemical Education 4(5), 583.

Dabit, A.S., Lianto, A.E., Branta, S.A., Laksono, F.B., Prabowo, A.R., Muhayat, N., 2020. Design of unmanned ships for fish feeding in coastal areas based on the arduino microcontroller. Mekanika 19, 74-82 (*In Indonesian*).

Das, S., 2014. Design and weight optimization of aluminum alloy wheel. International Journal of Scientific and Research Publications 4(6), 1-12.

Ghavidel, A., Rashki, M., Ghohani Arab, H. Moghaddam, M., A., 2020. Reliability mesh convergence analysis by introducing expanded control variates. Frontiers of Structural and Civil Engineering 14, 1012-1023.

Igbudu, S.O., Fadare, D.A., 2015. Comparison of loading functions in the modelling of automobile aluminum alloy wheel under static radial load. Open Journal of Applied Science 5, 403-413.

Ikhsan, Prabowo, A.R., Sohn, J.M., Triyono, J., 2020. Finite element analysis of different artificial hip stem designs based on fenestration under static loading. Procedia Structural Integrity 27, 101-108.

Karuppusamy, S., Karthikeyan, G., Dinesh, S., Rajkumar, T., Vijayan, V., Basha, K.J., 2016. Design and analysis of automotive wheel rim by using ansys and msc fatigue software. Asian Journal of Research in Social Sciences and Humanities 6, 196-212.

Kharmanda, G., 2016. Integration of multi-objective structural optimization into cementless hip prosthesis design: improved Austin-Moore model, Computer Methods in Biomechanics and Biomedical Engineering 19, 1557–1566.

Mohamad, M.L., Rahman, M.T.A., Khan, S.F., Basha, M.H., Adom, A.H., Hashim M.S.M., 2017. Design and static structural analysis of a race car chassis for formula society of automotive engineers (FSAE) event. Journal of Physics: Conference Series 908, 012042.

Muttaqie, T., Thang, D.Q., Prabowo, A.R., Cho, S.R., Sohn, J.M., 2019. Numerical studies of the failure modes of ring-stiffened cylinders under hydrostatic pressure. Structural Engineering and Mechanics 70, 431-443.

Nallusamy, S., Prabu, N.M., alakannan, K., Majumdar, G., 2015. Analysis of static stress in an alloy wheel of the passenger car. International Journal of Engineering Research in Africa 16, 17-25.

Prabowo, Bae, D.M., Sohn, J.M., 2019. Comparing structural casualties of the ro-ro vessel using straight and oblique collision incidents on the car deck. Journal of Marine Science and Engineering 7, 183.

Prabowo, A.R., Cao, B., Sohn, J.M., Bae, D.M., 2020. Crashworthiness assessment of thin-walled double bottom tanker: Influences of seabed to structural damage and damage-energy formulae for grounding damage calculations. Journal of Ocean Engineering and Science 5, 387-400

Ridwan, R., Prabowo, A.R., Muhayat, N., Putranto, T., Sohn, J.M., 2020. Tensile analysis and assessment of carbon and alloy steels using FE approach as an idealization of material fractures under collision and grounding. Curved and Layered Structures 7, 188-198.

Shah, C., 2002. Mesh discretization error and criteria for accuracy of finite element solutions. ANSYS Users Conference, 1-12.

Sureddi, C., 2018. Design, material optimization and dynamic analysis on automobile wheel rim. International Journal of Scientific and Research Publications 8, 486-509.

Wright, D.H., 1993. Testing Automotive Materials and Components. Warrendale (PA). SAE Publication.